Nonlinear optical effects in strain-induced laterally ordered (InP)$_2$/(GaP)$_2$ quantum wires

Y. Tang, H. T. Lin, and D. H. Rich*

Photonic Materials and Devices Laboratory, Department of Materials Science and Engineering, University of Southern California, Los Angeles, California 90089-0241

P. Colter and S. M. Vernon

Spire Corporation, Bedford, Massachusetts 01730

The nonlinear optical properties of a (InP)$_2$/(GaP)$_2$ bilayer superlattice structure have been examined with linearly polarized cathodoluminescence spectroscopy. Transmission electron microscopy showed a composition modulation with a period of ~800 Å along the [110] direction, which occurs spontaneously during the growth, resulting in coherently strained quantum wires. The strong excitation dependence of the polarization anisotropy and energy of excitonic luminescence from the quantum wires was found to be consistent with a band-filling model that is based on a **k·p** and two-dimensional quantum confinement calculation. [S0163-1829(96)51516-X]

Nonlinear optical properties of III-V semiconductor nanostructures have attracted a great deal of interest, as they are important for applications in optical communications that involve switching, amplification, and signal processing. An important nonlinear optical property is the change in the emission of light (in energy, polarization, and intensity) that results from phase-space filling of carriers in one- and two-dimensionally confined systems, i.e., quantum wells and wires.[1,2] This property is analogous to the Burstein-Moss band filling which occurs in bulk semiconductors and raises the energy of the unoccupied electron and hole states as the excitation intensity increases. As the dimensionality of the quantum confinement increases from one dimension (1D) to 2D, the narrowing of the density of states (DOS) will exhibit a lower excitation threshold for phase-space filling, thereby yielding potentially enhanced nonlinear optical effects. Recently, quantum wires have been fabricated by a strain-induced lateral ordering (SILO) process which occurs spontaneously when (GaP)$_n$/(InP)$_n$ and (GaAs)$_n$/(InAs)$_n$ short-period superlattices are grown on GaAs(001) and InP(001), respectively.[3–7] Previous studies involving transmission electron microscopy (TEM) and optical measurements such as photoluminescence, electroluminescence, and photoreflectance have shown evidence supporting the existence of quantum wires due to quantum confinement along both the growth direction and the composition modulation direction.[5–8] However, the nature of phase-space filling and the concomitant influence on the polarization properties in these systems have yet to be investigated thoroughly. In this study, we examine the nonlinear optical properties of a (InP)$_2$/(GaP)$_2$ bilayer superlattice (BSL) structure using a linearly polarized cathodoluminescence (LPCL) technique. We demonstrate the existence of an interesting excitation- and temperature-dependent polarization anisotropy in luminescence coming from the SILO quantum wires. A theoretical simulation of the band-filling, luminescence energy shifts and polarization anisotropy changes was performed for the SILO quantum wires using a **k·p** band-structure calculation, which takes the coherency strain and 2D quantum confine-

ment into account, and is compared with the experimental results. Evidence for these strong nonlinear optical effects is a cornerstone in establishing true quantum wire behavior and further underscores the good potential for applications in low-threshold lasers and exotic light modulators.

The BSL structure in this study was grown by metal-organic chemical-vapor deposition, and a schematic diagram is shown in Fig. 1. First, a 3000-Å In$_{0.49}$Ga$_{0.51}$P buffer layer was grown on a GaAs(001) substrate misoriented 3° toward (111)A. Each (InP)$_2$ and (GaP)$_2$ bilayer was grown in a time interval of ~10 sec, after which the system was purged to prepare for the succeeding layer. A total of 20 periods of (InP)$_2$/(GaP)$_2$ were grown giving a thickness of ~200 Å. Finally, a 3000-Å In$_{0.49}$Ga$_{0.51}$P capping layer was grown. Cross-sectional TEM revealed that the composition modulation occurred along the [110] direction with a period of ~800 Å. Previous reports on similar structures showed that the In composition varies from ~0.41 in the Ga-rich region to ~0.59 in the In-rich region.[8] Such a lateral superlattice embedded in an In$_{0.49}$Ga$_{0.51}$P barrier forms a multiple quantum wire array, as illustrated in Fig. 1.

The LPCL experiments were performed with a modified JEOL-840A scanning electron microscope using a 10-keV electron beam with a probe current I_b ranging from 50 pA to 30 nA. This CL system with polarization detection capability has been previously described.[9] The sample temperature was varied between 87 and 300 K, using a liquid nitrogen cryogenic specimen stage. Light with the electric field **E** parallel to the [110] or [1$\bar{1}$0] direction was detected. The luminescence signal was dispersed by a $\frac{1}{4}$-m monochromator and detected by a cooled GaAs:Cs photomultiplier tube with a spectral resolution of ~1 nm.

Polarized and nonpolarized CL spectra were taken as a function of probe current, as shown in Fig. 2 for a temperature of 87 K. In the wavelength range between 620 and 720 nm, two peaks originating from the BSL and In$_{0.49}$Ga$_{0.51}$P bulk (i.e., the buffer and capping layers) are observed. The peak energy of In$_{0.49}$Ga$_{0.51}$P bulk emission remains almost constant (~1.950 eV) for the different probe currents in Fig.
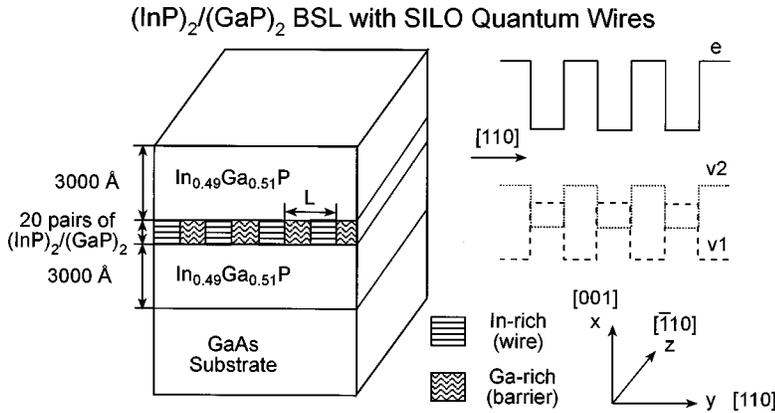
FIG. 1. A schematic diagram of the $(InP)_2/(GaP)_2$ BSL and type-I to type-II superlattice modulation for e-$v1$ and e-$v2$ transitions.

2. Emission from the BSL has a lower energy compared to that from the $In_{0.49}Ga_{0.51}P$ layers, as the lateral composition modulation along [110] results in ~ 400 Å$\times 200$ Å quantum wires composed of an In-rich $(GaP)_2/(InP)_2$ BSL region. The BSL peak energy shifts from 1.834 eV to 1.869 eV as I_b increases from 50 pA to 30 nA, as observed in Fig. 2 and plotted in Fig. 3. This highly nonlinear optical behavior shows that the confined states in the BSL can be filled by a fairly low electron-beam excitation. A narrower density of states is expected as the dimensionality of the quantum confinement increases from 1D to 2D. We suggest that the SILO formation of quantum wires in the BSL leads to the enhanced phase-space filling and nonlinear optical effects.

To further test this hypothesis, we have examined the polarization dependence of the luminescence in detail. The luminescence from $In_{0.49}Ga_{0.51}P$ bulk is polarized along the [110] direction and the magnitude of such polarization does not change for different probe currents and temperatures. This is consistent with a CuPt-like ordering which is found to occur along the $[\bar{1}11]$ or $[1\bar{1}1]$ direction of an epitaxially grown $In_{0.49}Ga_{0.51}P$ layer.[10] On the other hand, the polarization of emission from the BSL has an orthogonal orientation and greatly depends on the probe current and temperature, as shown in Figs. 2 and 4. With an increase in probe current from 50 pA to 30 nA, the polarization ratio $I_{\parallel}/I_{\perp}$, which is defined as the ratio of integrated CL intensities with electric field $\mathbf{E}$ parallel and perpendicular to the $[1\bar{1}0]$ quantum wire directions, reduces from ~ 1.5 to 1.1 at a temperature of 87 K. Under a fixed I_b, the polarization ratio decreases as the temperature increases, as shown in Fig. 4.

In order to model the nonlinear optical effects that are responsible for these polarization and energy changes, we have calculated the electron and hole eigenstates of the BSL using a single-band effective-mass approximation with band parameters found using the $\mathbf{k \cdot p}$ perturbation method employing a full Luttinger-Kohn and Pikus-Bir Hamiltonian.[11] The BSL is assumed to be coherently strained so that its in-plane lattice constant, $a_{\parallel}$, is equal to that of GaAs. Assuming a biaxial strain on the (110) interfacial plane between In-rich and Ga-rich regions, we obtain the strain tensor in the $\langle 100 \rangle$
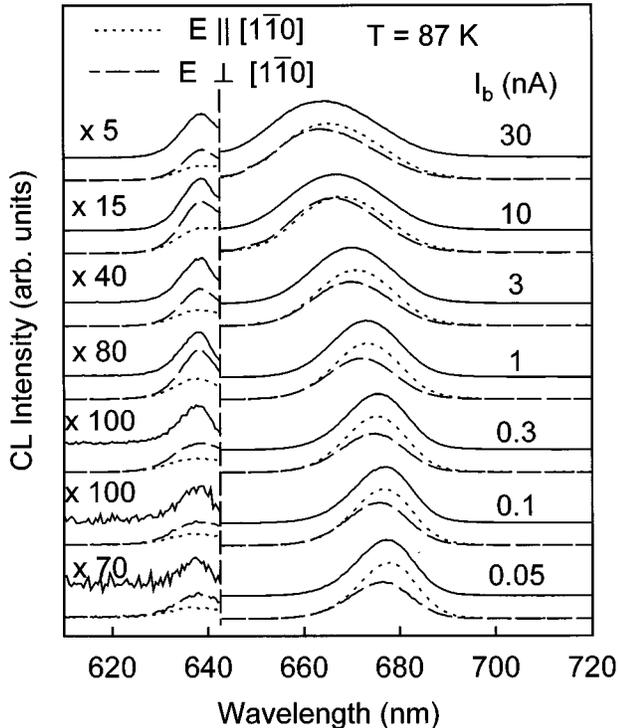
FIG. 2. Stack plots of normalized spatially integrated nonpolarized (solid line) and polarized (dashed lines) CL spectra taken for different probe currents at $T = 87$ K.
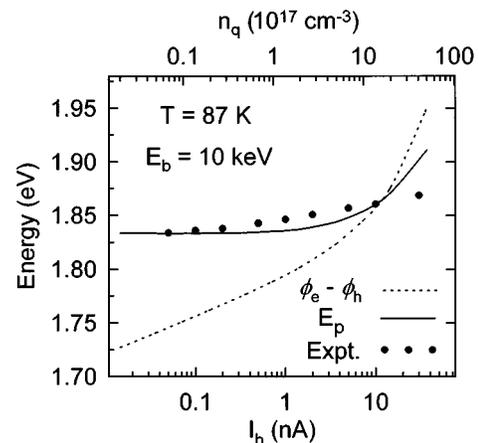
FIG. 3. Experimental and calculated energies of the peak CL intensity position, E_p, and calculated quasi-Fermi-level difference vs the excitation density and probe current.
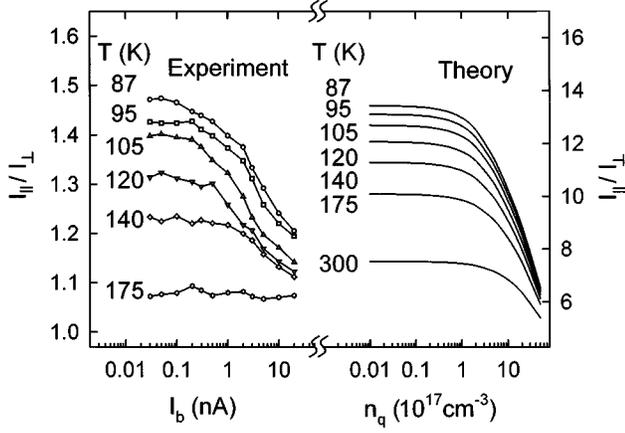
FIG. 4. Experimental and theoretical polarization ratios, $I_\parallel/I_\perp$, as a function of the excitation density. Parallel and perpendicular subscripts are defined with respect to the $[1\bar{1}0]$ quantum wire direction.

representation for each $In_xGa_{1-x}P$ (x=0.41 or 0.59) region of the BLS as follows:

$$\varepsilon_{11}=\varepsilon_{22}=\frac{2C_{44}-C_{12}}{C_{11}+C_{12}+2C_{44}}\,\varepsilon_\parallel,$$

$$\varepsilon_{12}=-\frac{C_{11}+2C_{12}}{C_{11}+C_{12}+2C_{44}}\,\varepsilon_\parallel, \qquad (1)$$

$$\varepsilon_{23}=\varepsilon_{31}=0,\quad \varepsilon_{33}=\varepsilon_\parallel,$$

where C_{11}, C_{12}, and C_{44} are elastic stiffness constants of $In_xGa_{1-x}P$, $\varepsilon_\parallel=(a_\parallel-a_i)/a_i$ is the (001) in-plane strain, and a_i is the unstrained lattice constant for either the In- or Ga-rich regions of the BSL, using a pseudoalloy approximation. The Luttinger parameters, deformation potentials, elastic constants, and spin-orbit splitting were approximated using a linear interpolation between values which are known for GaP and InP.[8] The diagonalization of the Hamiltonian results in the E vs $\mathbf{k}$ bulk-band dispersion for electrons and holes and enables a determination of the set of strain-split valence-band Bloch functions, which contain admixtures of the $|\frac{3}{2},\pm\frac{3}{2}\rangle$, $|\frac{3}{2},\pm\frac{1}{2}\rangle$, and $|\frac{1}{2},\pm\frac{1}{2}\rangle$ states, owing to the magnitude and low symmetry of the strain. The conduction- to valence-band offset ratio ($\Delta E_c/\Delta E_v$) is taken as 75/25, and is assumed independent of the alloy composition.[12] This results in type-I and type-II superlattices for the two uppermost valence bands, $v1$ and $v2$, in the In- and Ga-rich regions, respectively, which have characters that are 96% heavy-hole (hh; $m_j=\pm\frac{3}{2}$) and 94% light-hole (lh; $m_j=\pm\frac{1}{2}$) in the $\langle110\rangle$ representation. Other salient features of the calculation are that $\Delta E_c=120$ meV, $\Delta E_v=40$ meV for the $v1$ bands, and $v1$ and $v2$ are split by 42 and 48 meV in the In- and Ga-rich regions, respectively. Since e-$v1$ and e-$v2$ transitions are spatially direct and indirect transitions, respectively, the relative contribution of e-$v1$ and e-$v2$ optical transitions should involve an interplay between the electron-hole wave function overlap and carrier occupation density. The e-hh and e-lh transitions, in strained and quantum confined systems, will generally exhibit an orthogonal polarization dependence. By altering the relative contributions of the e-$v1$ and e-$v2$ tran-

sitions in the luminescence, which can be accomplished by changing the excitation density (i.e., probe current here), a variation in the polarization ratio is thus expected. In order to analyze quantitatively the excitation-dependent polarization anisotropy, we first need to calculate the eigenstates in the quantum wires.

The electron and hole envelope wave functions $\Psi_{e,h}(x,y)$ in the quantum wire are determined by solutions to the 2D Schrödinger equation,

$$\left[-\frac{\hbar^2}{2m^*_{e,h}(x,y)}\left(\frac{\partial^2}{\partial x^2}+\frac{\partial^2}{\partial y^2}\right)+V_{c,v}(x,y)\right]\Psi_{e,h}(x,y)$$
$$=E_n^{e,h}\Psi_{e,h}(x,y), \qquad (2)$$

where $m^*_{e,h}(x,y)$ is the electron or hole effective mass, $V_{c,v}(x,y)$ is the effective conduction- and valence-band confinement potential, and $E_n^{e,h}$ is the nth eigenstate energy. The distances along [001] and [110] are represented by x and y, respectively (as in Fig. 1). The shape of the actual potential is complicated and some uncertainties remain, so a simplified treatment is employed using a rectangular approximation to the potential profile $V_{c,v}(x,y)$. This potential profile and effective masses for electrons and holes were determined by the $\mathbf{k}\cdot\mathbf{p}$ calculation discussed above. We assume a negligible coupling between orthogonal eigenstates, i.e., $\Psi_{e,h}(x,y)\approx\Psi_{e,h}(x)\Psi_{e,h}(y)$, as can be verified for a relatively large dimension quantum wire (greater than $\sim100\times100$ Å^2).[13] Equation (2) can then be separated into two coupled differential equations for x and y. The quantized energy levels, $E_n^{e,h}$, can be solved separately for the two confinement directions as $E_n^{e,h}=E_{x,i}^{e,h}+E_{y,j}^{e,h}$, using a transfer matrix method.[14]

Using these eigenstates, quasi-Fermi energies for electrons and holes can be determined for a given excess carrier concentration, n_q, to examine the band filling. The electron and hole carrier densities, $n_i^{e,h}$, in these quantized states can be determined by integrating the product of the 1D density of states and the Fermi-Dirac function, $f(E-\phi_{e,h})$, for electrons and holes. The quasi-Fermi levels, $\phi_{e,h}$, are determined by solutions of the following equations:

$$n_i^{e,h}=\int_{E_i}^\infty\frac{dE}{\pi L_x L_y}\left(\frac{2m_z^{e,h}}{\hbar^2}\right)^{1/2}\frac{f(E-\phi_{e,h})}{\sqrt{E-E_i^{e,h}}},$$
$$\qquad (3)$$

$$n_q=\sum_i n_i^e=\sum_i n_i^h,$$

where L_x and L_y are the dimensions of the quantum wire, and $m_z^{e,h}$ is the effective mass along $[1\bar{1}0]$ (z direction). The difference between the quasi-Fermi energies of electrons and holes is shown in Fig. 3 as a function of the probe current. In this calculation all bound states were included and resulted in 21 electron, 45 $v1$, and 20 $v2$ states. As the quasi-Fermi-level difference increases with increasing probe current, optical transitions with higher energies contribute to the luminescence spectrum, resulting in the observed blueshift in the BSL peak. The luminescence line shape $I(\hbar\omega)$ can further be calculated from

$$I(\hbar\omega) = \sum_{ij} I_{ij}^2 \int_{E_i^e}^{\hbar\omega - E_g - E_j^h} dE \; H(\hbar\omega - E_g - E_i^e - E_j^h)$$

$$\times g_J(\hbar\omega) f(E - \phi_e) f(\hbar\omega - E_g - E - \phi_h),$$

$$g_J(\hbar\omega) = \frac{1}{\pi\sqrt{2}\hbar} \frac{\sqrt{m_r}}{\sqrt{\hbar\omega - E_g - E_i^e - E_j^h}}, \qquad (4)$$

where $H(E)$, the Heaviside function, is 0 for $E < 0$ and is 1 for $E \geq 0$, I_{ij} is the overlap integral for electron and hole envelope wave functions, i.e., $I_{ij} = \int d^2\mathbf{r}\,\Psi_{i,e}(x,y)\Psi_{j,h}(x,y)$, and $g_J(\hbar\omega)$ is the joint density of states for k_z-conserving interband transitions in quantum wires, which contains the reduced mass term m_r, where $1/m_r = 1/m_z^e + 1/m_z^h$. Using the calculated values for the quasi-Fermi levels, we have calculated $I(\hbar\omega)$ as a function of carrier density. In addition, to include the effects of instrumental and inhomogeneous broadening, we have convolved $I(\hbar\omega)$ with a Gaussian of width equal to the width of the narrowest optical transition, which was measured for the lowest probe current of 50 pA in Fig. 2. The position of maximum peak intensity of $I(\omega)$, E_p, is plotted versus n_q in Fig. 3, and shows a reasonable agreement with the experimental BSL peak position.

We have further calculated the polarization dependence of the luminescence from the BSL as a function of excitation density. Since $g_J(\hbar\omega)$ is singular for the lowest-energy optical transitions, the largest polarization anisotropy is dominated by states with $k_z = 0$, which occur for the lowest excitation conditions. From the overlap integrals, I_{ij}, and the calculated conduction and valence Bloch functions, we can calculate the polarization-dependent transition matrix elements. The integrated intensity of polarized luminescence is determined by the carrier occupation densities and the electron-hole wave-function overlap according to

$$I_{\perp,\parallel} = \sum_{i,j} n_i^e n_j^h |I_{ij}\langle u_{i,c}|\mathbf{E}_{\perp,\parallel} \cdot \mathbf{p}|u_{j,v}\rangle|^2, \qquad (5)$$

where $\mathbf{E}_{\perp,\parallel}$ is the electric field of emitted light which is detected either along the [110] ($\perp$) or [1$\bar{1}$0] ($\parallel$) direction, $\mathbf{p}$ is the linear momentum operator, and $u_{i,c}$ and $u_{j,v}$ are the set of band-edge conduction- and valence-band Bloch functions, the latter of which is a linear combination of the six $|J, m_j\rangle$ states in the $\langle 110\rangle$ representation as determined from the above $\mathbf{k}\cdot\mathbf{p}$ calculation. The calculated polarization ratio $I_{\parallel}/I_{\perp}$ is shown in Fig. 4 as a function of probe current and carrier concentration,[15] and is compared with the experimental results. The general features of the experiment and theory are quite consistent,[16] regarding the excitation-induced reduction in polarization anisotropy, and thus confirm that our phase-space filling and SILO quantum wire model reasonably explains the nonlinear optical behavior observed in the LPCL data.

In conclusion, we have performed a detailed study of the band-filling and polarization anisotropy of an $(InP)_2/(GaP)_2$ BSL using linearly polarized CL. We have calculated the excitation-dependent polarization anisotropy and CL energy shifts with a $\mathbf{k}\cdot\mathbf{p}$ model that incorporates both strain and quantum confinement. The calculations confirm a strong interplay between band-filling and e-h wave-function overlap, which leads to very interesting and possibly useful nonlinear optical and polarization properties.

---

*Author to whom correspondence should be addressed.

[1] S. Schmitt-Rink, D. S. Chemla, and D. A. B. Miller, Adv. Phys. **38**, 89 (1989).

[2] V. D. Kulakovskii, E. Lach, and A. Forchel, Phys. Rev. B **40**, 8087 (1989).

[3] K. C. Hsieh, J. N. Baillargeon, and K. Y. Cheng, Appl. Phys. Lett. **57**, 2244 (1990).

[4] K. Y. Cheng, K. C. Hsieh, and J. N. Baillargeon, Appl. Phys. Lett. **60**, 2892 (1992).

[5] P. J. Pearah, E. M. Stellini, A. C. Chen, A. M. Moy, K. C. Hsieh, and K. Y. Cheng, Appl. Phys. Lett. **62**, 729 (1993).

[6] A. C. Chen, A. M. Moy, P. J. Pearah, K. C. Hsieh, and K. Y. Cheng, Appl. Phys. Lett. **62**, 1359 (1993).

[7] P. J. Pearah, A. C. Chen, A. M. Moy, K. C. Hsieh, and K. Y. Cheng, IEEE J. Quantum Electron. **30**, 608 (1994).

[8] A. Mascarenhas, R. G. Alonso, G. S. Horner, S. Froyen, K. C. Hsieh, and K. Y. Cheng, Phys. Rev. B **48**, 4907 (1993).

[9] D. H. Rich, A. Ksendzov, R. W. Terhune, F. J. Grunthaner, B. A. Wilson, H. Shen, M. Dutta, S. M. Vernon, and T. M. Dixon, Phys. Rev. B **43**, 6836 (1991).

[10] A. Mascarenhas, S. Kurtz, A. Kibbler, and J. M. Olson, Phys. Rev. Lett. **63**, 2108 (1989).

[11] F. H. Pollak, in *Semiconductors and Semimetals*, edited by R. K. Willardson and A. C. Beer (Wiley, New York, 1990), Vol. 32, pp. 17–53.

[12] R. P. Schneider, Jr., R. P. Bryan, E. D. Jones, and J. A. Lott, Appl. Phys. Lett. **63**, 1240 (1993).

[13] K. B. Wong, M. Jaros, and J. P. Hagon, Phys. Rev. B **35**, 2463 (1987).

[14] B. Jonsson and S. T. Eng, IEEE J. Quantum Electron. **26**, 2025 (1990).

[15] The relationship between n_q and I_b is given by $n_q \approx 2I_b E_b \tau_r / (3eE_g \pi r_e^2 T_{BSL})$, where E_b is the e-beam energy, E_g is the $In_{0.49}Ga_{0.51}P$ band gap and is 1.950 eV, r_e is the lateral radius of e-h excitation, τ_r is the e-h lifetime, and $T_{BSL} = 200$ Å, the BSL thickness. Using $r_e \approx 0.5$ μm and $\tau_r \approx 0.1$ ns [from M. Prasad *et al.*, J. Electron. Mater. **23**, 359 (1994)] we get n_q (cm^{-3}) = $1.36 \times 10^{17} I_b$ (nA).

[16] Deviations between experiment and theory can largely be traced to the optical collection system used in the experiment, as the ellipsoidal mirror causes a polarization mixing that results in a maximum of $I_{\parallel}/I_{\perp} \sim 4$, as discussed in Ref. 9.